

Finite Element Model for Pull-Out Test of Reinforcement Embedded in Confined Concrete

Muhd Fauzy Sulaiman¹, Chau-Khun Ma^{2*}, Nazirah Mohd Apandi³,
Chee-Loong Chin⁴, Kee-Hong Ler⁴

¹ Civil Engineering Program, Faculty of Engineering,
Universiti Malaysia Sabah, Kota Kinabalu, 88400, MALAYSIA

² Forensic Engineering Centre, Institute for Smart Infrastructure and Innovative Construction,
Faculty of Civil Engineering,
Universiti Teknologi Malaysia, Skudai, 81310, MALAYSIA

³ Department of Structure and Materials, School of Civil Engineering, College of Engineering,
Universiti Teknologi MARA, Shah Alam, 40450, MALAYSIA

⁴ Department of Structure and Materials, Faculty of Civil Engineering,
Universiti Teknologi Malaysia, Skudai, 81310, MALAYSIA

*Corresponding Author: machaukhun@utm.my

DOI: <https://doi.org/10.30880/ijie.2025.17.09.026>

Article Info

Received: 11 January 2025

Accepted: 26 August 2025

Available online: 31 December 2025

Keywords

Finite Element Analysis (FEA),
reinforced concrete (RC), pullout
test, concrete damaged-plasticity
(CDP) model, SSTT-confinement

Abstract

A finite element (FE) model was developed to simulate the pull-out test of steel rebar embedded in concrete confined with pre-tensioned steel straps. The model treated both the concrete and steel rebars as refined solid elements, enabling explicit representation of their deformations. A surface-to-surface contact model was employed at the concrete-rebar interface to ensure accurate load transfer. The importance of using a confined concrete model capable of accurately simulating nonlinear behavior under high confining pressures was emphasized in the modelling process. For this purpose, the concrete damaged-plasticity (CDP) model was adopted. Multiple pull-out tests were simulated using this approach, and comparisons with experimental data demonstrated that the proposed FE model accurately reproduced bond stress-slip responses. Additionally, the model successfully captured different failure modes, including splitting failure in specimens without confinement and pull-out failure in confined specimens.

1. Introduction

Reinforced concrete (RC) is a composite structural material consisting of reinforcing steel embedded within concrete [1]. For effective composite action, proper force transfer between concrete and steel, known as bond, is essential [2]. Traditionally, the pull-out test has been the standard method for studying RC bond behavior. This includes examining the bond-zone load transfer mechanism, factors influencing bond strength, and the bond stress-slip relationship [3]. In the test, a single ribbed bar with a short embedment length is embedded in a concrete cylinder and pulled out until the specimen fails. The short embedment length ensures a uniform bond stress distribution along the bonded area, allowing for the accurate measurement of pure bond force [4].

External confinement methods are effective techniques for increasing the bond strength between concrete and reinforcement by applying external pressure [5] – [8]. There are lots of confinement techniques that are used for strengthening or rehabilitating concrete, including concrete-filled steel tube, steel jacketing, concrete jacketing, steel strapping tensioning technique (SSTT), fiber-reinforced polymer (FRP) confinement, and so on [9] – [11]. Among these methods, SSTT has emerged as a particularly effective approach. SSTT had been proven to

have the ability to enhance bond strength by actively confining concrete, preventing it from dilating and debonding from the reinforcement [5] – [7]. Generally, SSTT is an active confinement method that involves tensioning steel straps around concrete to apply external pressure, significantly enhancing the mechanical properties of the confined concrete [10], [12], [13].

Previous studies extensively focused on modelling the bond and anchorage behavior of confined concrete, particularly using FRP-confined concrete as a predictive model [14] – [16]. However, the modelling approach for FRP confinement is not applicable to predicting bond behavior in confined concrete using prestressed steel strap due to the distinct nature of the confinement (passive confinement versus active confinement) [12], [17]. The expression for the confining pressure gradient in SSTT (active confinement) differs significantly from that proposed for passive confinement using FRP in terms of lateral strain-axial strain and axial stress-strain behavior [12], [18], [19].

Currently, no model has been developed for active confinement, particularly SSTT confinement. The materials used and the active confining pressure of active confinement on concrete would be considered in this research. This research is the first to explore a modelling approach for SSTT-confined concrete concerning bond and anchorage behavior. However, the approach is constrained by the limited availability of resources and reference data, making it less comprehensive compared to other numerical models. In developing the 3D finite element (FE) model, several assumptions were made to ensure a cohesive and consistent approach. The material properties of all sub-models, including the concrete block, steel bar, and steel straps, were assumed to be isotropic. A perfect bond was considered at the interface between the concrete and the steel bar, ensuring seamless force transfer. Additionally, the pre-tensioned confinement exerted on the concrete surface was assumed to be uniform and perfectly applied across the entire surface.

2. Research Methodology

2.1 Element Types and Geometry

The geometry of specimens is the same as the geometry of the specimens used in experimental studies where the concrete block was dimensioned 150 mm in diameter and 300 mm in height. The steel reinforcement used was 16 mm in diameter and steel straps were 0.5 mm in thickness and 15 mm in width. Non-linear analyses were used in the study and asymmetry simplification of the model was implemented. For meshing purposes, the concrete block was divided into several parts. This is to ensure an accurate contact stimulation of the contact zone between the concrete and ribbed bar as well as between the concrete and steel straps. Fig. 1 shows the meshing of the proposed model.

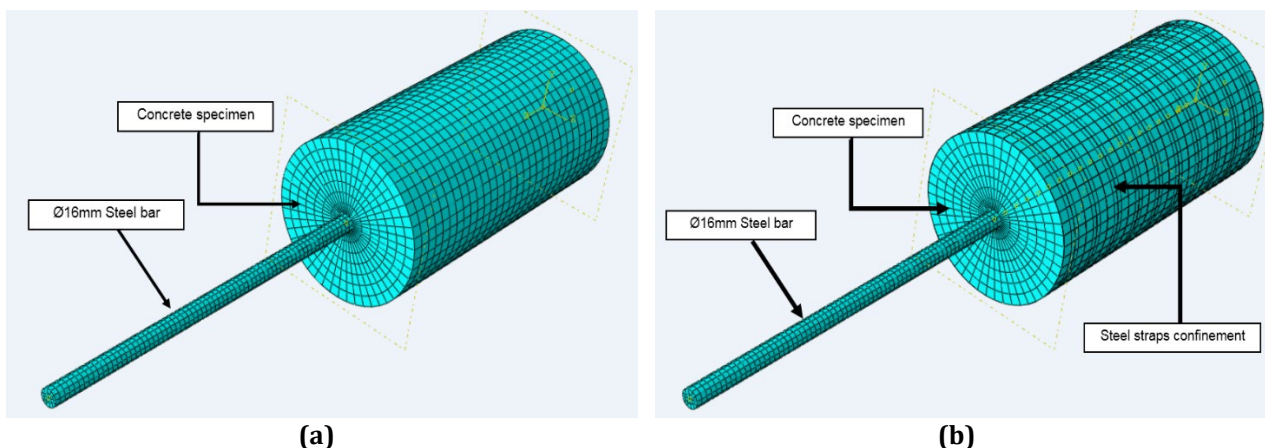


Fig. 1 Meshing of proposed models (a) Meshing of FE model; (b) Meshing of FE model with steel straps

For generating a mesh of concrete block, ribbed bars and steel straps, the hexahedral elements with 8-nodes were used in the study. These are the iso-parametric elements developed by a tensor product Gauss quadrature rule. In order to determine the influence of the mesh to refinement on the results, a convergence test was conducted. The results of the convergence test are depicted in Table 1, and Fig. 2 illustrates the convergence curve of meshing sizes.

From the convergence test conducted, the bond strength, τ of FE model was not varied much when the meshing size of 10 and less in sizes. Moreover, the slip measurement also not affected when the meshing of 10 and reduced has been used inside the proposed mode. This test results indicated that the meshing sizes were not

affected by the model when a mesh size of 10 or less was used. Therefore, in this case, the global sizes of meshing (10) are used for development of FE model.

Table 1 Results of the convergence test

| Properties | Global Size | | | | |
|---------------|-------------|----------|----------|----------|----------|
| | 20 | 15 | 10 | 8 | 5 |
| Maximum Force | 130.3031 | 129.8806 | 129.5116 | 129.5116 | 129.5116 |
| Bar slip | 25.3729 | 24.9853 | 24.3561 | 24.3561 | 24.3561 |

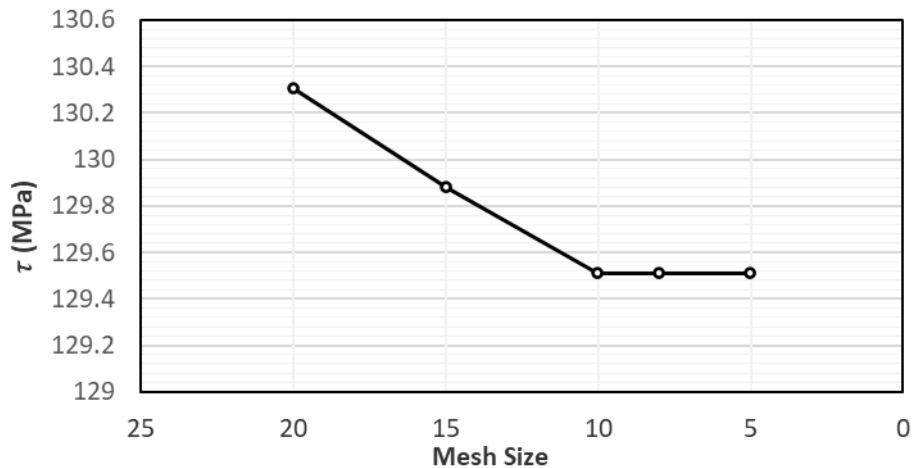


Fig. 2 Convergence curve of meshing sizes

2.2 Properties of Materials

In this study, an elastic-plastic model was used to model the pull-out behavior. The elastic-plastic model is the simplest model that considers the elastic and plastic properties of materials for bond prediction. All the previous models are using this model to develop their bond models. Moreover, this model also allows the user to define the bond interaction between embedded region as well as between confined material and concrete substrate. This interaction definition is necessary in bond model as to connect all the sub-models into total models before the model can be used for bond predictions. If the interaction between sub-models were incorrect, then the model could not be used, and the user needs to define it again.

The mechanical properties of the materials used are obtained from the series of experimental tests. The concrete properties that have been used in this model is normal mixed for high-strength concrete (HSC), where the properties of concrete G60 with Young Modulus, $E = 29$ GPa and Poisson ratio, $\nu = 0.2$ [20]. Furthermore, the isotropic type of elastic-plastic also required the plastic behavior of concrete beyond the elastic regions. The yield strength, as well as plastic strains, was also obtained through the series of experimental tests in the laboratory. The ribbed bars and steel straps properties are also gained through the experimental works reported by Sulaiman et al. [7] where the E obtained are 219 GPa and 220 GPa, respectively.

The model analyses were conducted by applying displacement imposed by allowing for control of post-peak behavior. This is to ensure the final iteration process was performed well to get good FE analyses.

2.3 Modelling Interfaces for Proposed Model

In the model, there are two interfaces interaction that have been identified, which are the interfaces between: (1) concrete and ribbed bars, and (2) concrete and steel straps. Currently, there are very limited studies regarding bond-slip models. The embedded interface between ribbed bar and concrete considers contact properties of cohesive behavior.

In cohesive behavior, the traction separation behavior needed to be identified for the element separations. The parameters used for maximum cohesive stress are set to 10 MPa while the fracture energy is 0.15 N/mm as reported in Sulaiman *et al.* [5]. Moreover, the embedded region of ribbed bar must be separated from surround concrete by implementing traction separation parameters for FE analyses. The referred traction separation parameters specified to cohesive behavior under normal directions as well as tangential directions as for the response to bond-slip models. Most of the previous models are using these types of interface interactions to ease

the user to define the suitable interface for their proposed bond model. As reported by Sulaiman *et al.* [5], the surface-to-surface contact interaction was defined between the concrete and the embedded steel bar. Tangential behaviors with friction coefficient of 0.4 was used, based on literature for concrete to steel bar interface. This will be allowing the model to simulate bond degradation and pull-out behavior, allowing the steel bar to slide out for capturing bond behavior of confined concrete. For the ribbed steel bar, it is not explicitly modeled with its physical rib geometry. Instead, the ribbed effects were implicitly accounted as a cohesive surface interaction which is the tangential behavior of friction coefficient. In this model, tangential behavior is represented as the frictional resistance between concrete and steel bar. The cohesive properties ensure the influence of rib geometry on bond strength between concrete to steel bar. This approach is commonly used in FE modelling when the actual ribs are too small to be efficiently meshed or modeled explicitly while preserving accuracy in predicting bond-slip responses.

Meanwhile, most of the studies are focused on CFRP and FRP confinement, where there is a very lack of knowledge regarding steel strap confinements. According to Arruda *et al.* [21], the bond between concrete and confinements were stimulated by interface contacts. The interface stimulation was normal behavior by considering contact stiffness between two mediums whereas in this study the interface is between concrete surfaces and steel straps confinement.

3. Results and Discussion

This section discussed the comparison between experimental results as well as the numerical model results for bond-slip behavior. The experimental results used were obtained from the study conducted by Sulaiman *et al.* [7]. The proposed model is the very first developed FE model with inclusion of confining ratio, ρ_v , whereas none of existing bond-slip models are considering the effects of SSTT confinement on bond-slip behavior of confined concretes. According to Sulaiman *et al.* [7], the designations of specimens were designed into: (1) types of confinement, (2) concrete strength, (3) diameter of rebar, and (4) embedment length of the specimens. For instance, pull-out specimen of SS-G60-12-80, the specimen has the following properties: (1) SSTT fully confinement, (2) concrete strength of 60 MPa, (3) 12 mm bar diameter, and (4) 80 mm of embedment length. From the developed model, it is shown that the steel straps confinement has been proven to give confinement on concrete and contributed to the enhancement of bond behaviors of confined specimens. Fig. 3 depicts the stress distribution of proposed model along the concrete specimen.

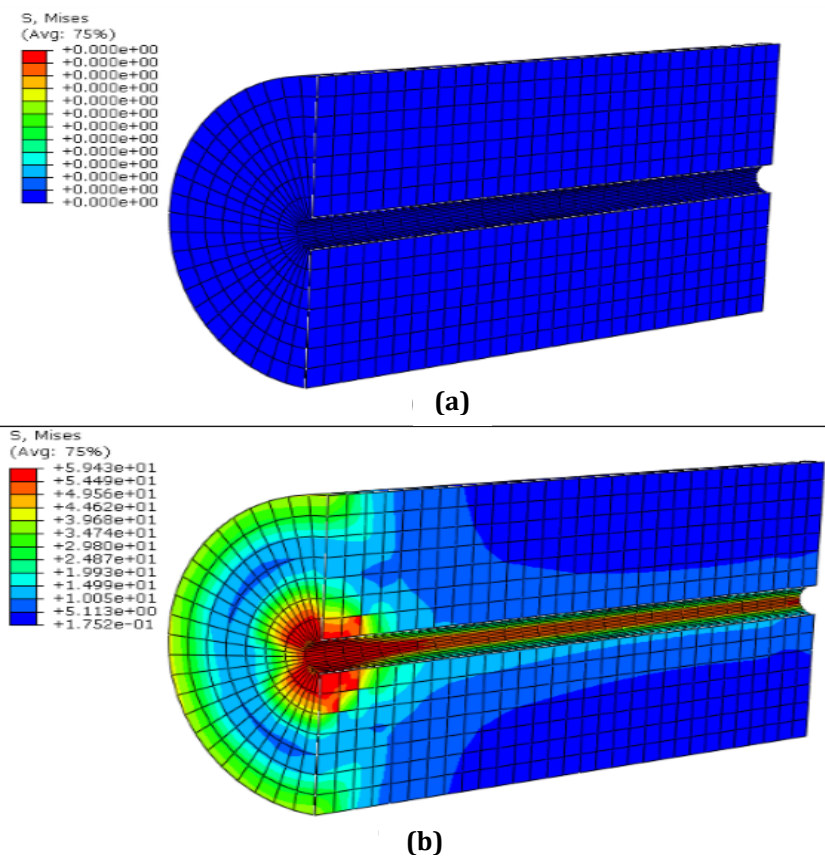


Fig. 3 Stress distributions of the concrete specimen under two conditions which are (a) Normal condition; (b) Pull-out condition

Fig. 4 shows the stress revolutions of proposed model. From Fig. 4, the stress distribution of the concrete specimen was observed. During pull-out test, the contact between concrete and ribbed bars was under friction due to induce τ . During normal conditions as illustrated in Fig. 4a, there is no stress observed as the concrete and ribbed bar are in static condition. As the bar was being pulled out from the concrete, friction was induced between these two mediums. Initially, the stresses were observed at the location where the ribbed bar was being pulled out from concrete specimen. Then, the stress slowly propagated along the embedment length of bar as the it continued to be pulled out. This situation continues until the pull-out specimens have failed. Fig. 5 illustrates the comparison between proposed model and pull-out specimen.

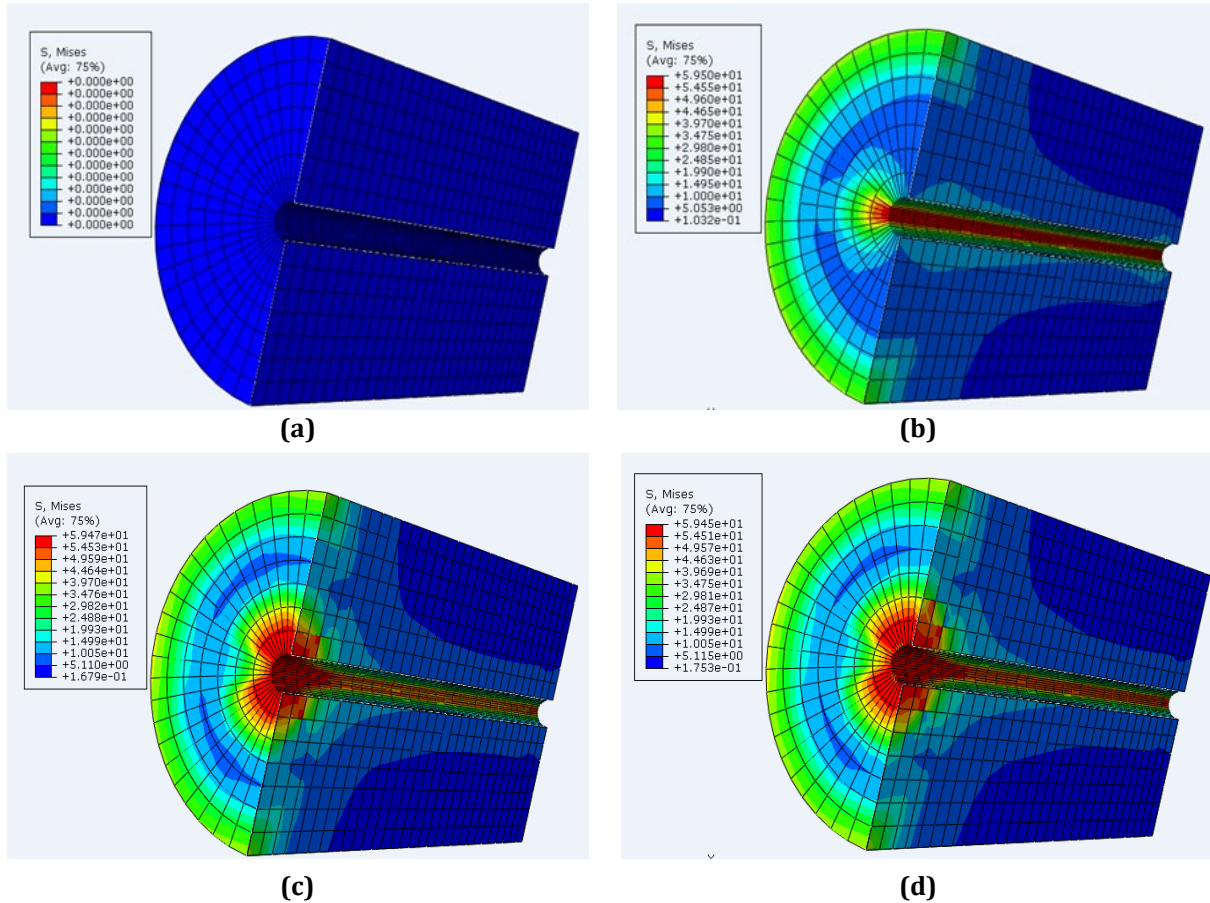


Fig. 4 Stress revolutions of proposed model (a) Static Load; (b) Load = 30% of P_{max} ; (c) Load = 70% of P_{max} ; (d) Load = P_{max}

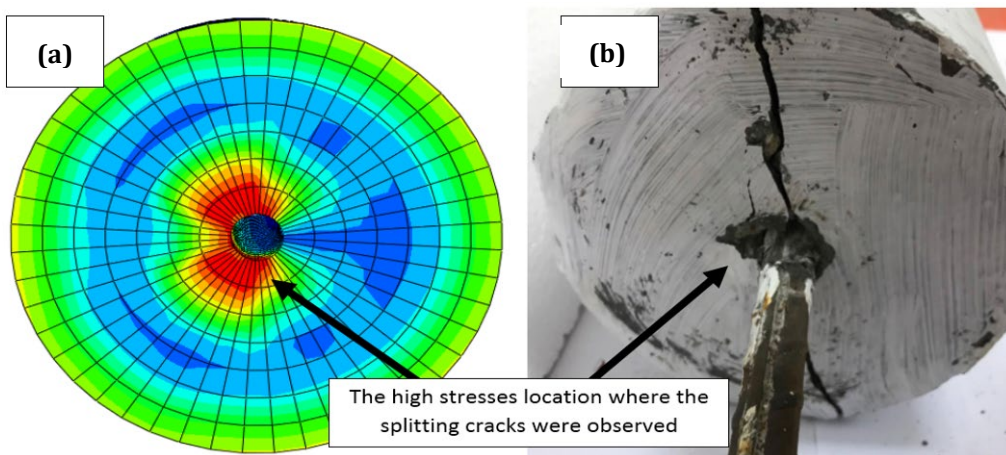


Fig. 5 The high stresses location of (a) proposed model; and (b) pull-out specimen

In Fig. 5, the stress distributed highest at the location where the ribbed bar is being pulled out. At this location, the stresses were focused on the inner location of the concrete specimen. The stresses were formed due to the reaction from pull-out of ribbed bar. Then, the stress slowly forms micro-cracks at this location. As the pulling continued, the cracks became bigger and formed splitting cracks. Therefore, the requirement of confinement is necessary to prevent the formation of splitting cracks which may lead to total bond and anchorage failures in RC structures. Table 2 shows the comparison between developed models and experimental data of pull-out specimens.

Table 2 Comparison between developed model and pull-out experimental data

| Specimens | P_{max} (kN) | τ (MPa) | Post-peak Load (kN) | Load Reduce (%) | Ultimate Load slip (mm) | Maximum slip (mm) | Differences in slip (%) |
|-------------------------------------------|-------------------|-----------------|------------------------|-----------------------|-------------------------------|----------------------|----------------------------|
| Proposed Model for 0 mm spacing | 132.0 | 8.75 | 120.70 | 8.5 | 23.95 | 30.30 | 20.95 |
| SS-G60-16-300 | 133.0 | 8.86 | 101.52 | 23.6 | 23.34 | 31.12 | 25.00 |
| Proposed Model with 10 mm spacing | 130.1 | 8.63 | 117.50 | 9.68 | 24.15 | 30.85 | 21.71 |
| SS10-G60-16-300 | 131.9 | 8.75 | 106.30 | 19.40 | 24.26 | 32.10 | 24.42 |
| Proposed Model with 20 mm spacing | 129.5 | 8.59 | 114.40 | 11.66 | 24.35 | 32.40 | 24.84 |
| SS20-G60-16-300 | 130.9 | 8.68 | 99.60 | 23.96 | 26.30 | 36.65 | 28.24 |
| Proposed model for unconfined concrete | 129.0 | 8.55 | 115.60 | 10.39 | 26.42 | 35.30 | 25.16 |
| Cont-G60-16-300 | 131.0 | 8.62 | 90.00 | 31.29 | 26.55 | 37.20 | 28.62 |

From Table 2, it is indicated that the P_{max} for proposed model and control model about 1.0% and 1.5% less compared to SS-G60-16-300 and Cont-G60-16-300, respectively. The predicted τ for is approximately similar compared to the experimental data. Meanwhile, the maximum bar slip recorded for proposed model and control model is about 2.7% and 5.3% less SS-G60-16-300 and Cont-G60-16-300, respectively. The behavior of developed bond-slip models has not varied much compared to pull-out specimens whereas the implementation of experimental parameters has been included for the development of FE models. These parameters are important to determine the behavior of the proposed model, especially regarding the SSTT-confined model.

With the effect of confinement ratio, ρ_v , the proposed model exhibited 10% higher of post-peak bond strength compared to SS-G60-16-300. The experimental post-peak bond strength of SS-G60-16-300 was 18% lower compared to the proposed model. There are many possibilities that contributed to differences in post-peak of τ between proposed model and SS-G60-16-300, one of them is an improper vibration during concrete cast. If vibration of concrete was not done well, the presence of voids will reduce the concrete strength, f_{cu} as well as bond between rebar and concrete. The voids will technically reduce the surface contact between surround concrete and RB which tends to ease the bar to slip during pull-out tests.

The post-strength of Cont-G60-16-300 has reduced 23.6% from the ultimate bond strength meanwhile, the control model has reduced 8.5% compared to the ultimate strength, respectively. The present of SSTT confinement in proposed model has significantly decreased the bar slip of confined concrete. From the table, the control model indicated 25.16% differences of slip meanwhile the proposed model indicated 20.95%. The bar-slip of the proposed model significantly reduced to 5% from ultimate strength to post-strength of confined concrete. Furthermore, it was observed that the proposed model slightly overestimates the post-peak bond strength compared to experimental results. This may be due to modelling simplifications and the inherent assumptions of the CDP model under high confinement. Therefore, the post-peak predictions from the FE model should be conservatively interpreted when applied to structural design.

The provision of confining pressure by SSTT has significantly increased the bond mechanisms between concrete and RBs, hardened the bar from easily slip and enhanced τ up to 10%. By comparing the proposed model with the control model, the P_{max} of the proposed model was 5% higher compared to the control model. Meanwhile, the comparison of the P_{max} of Cont-G60-16-300 with SS-G60-16-300 indicated the P_{max} about 3% differences between these them. It is not much varied for τ of the experimental results and developed models as the same experimental data were used to develop the models.

For the proposed model with 10 mm spacing, the predicted P_{max} was about less than 3% difference between SS10-G60-16-300. The developed model has predicted that the τ approximately equal to the SS10-G60-16-300. In addition, the ultimate slip was about 5% difference between them.

Fig. 6 indicates the typical bond-slip curves of proposed models and pull-out specimens. From Fig. 6, the proposed model exhibited the stiffest of the elastic region among four bond-slip curves observed. As illustrated, the inclusion of ρ_v up to 0.152 has increased the elastic properties of confined concrete by about 5% compared to control. Moreover, the proposed model curve has lined along together with the bond-slip curve of SS-G60-16-300 and not vary much from the experimental bond-slip curve. The proposed model has predicted bond-slip curves of confined concrete are approximately same with experimental results of confined pull-out specimen. Hence, the proposed model can be used to predict the bond-slip curves under confinement effects. Fig. 7 to 10 show the bond-slip curves of proposed models.

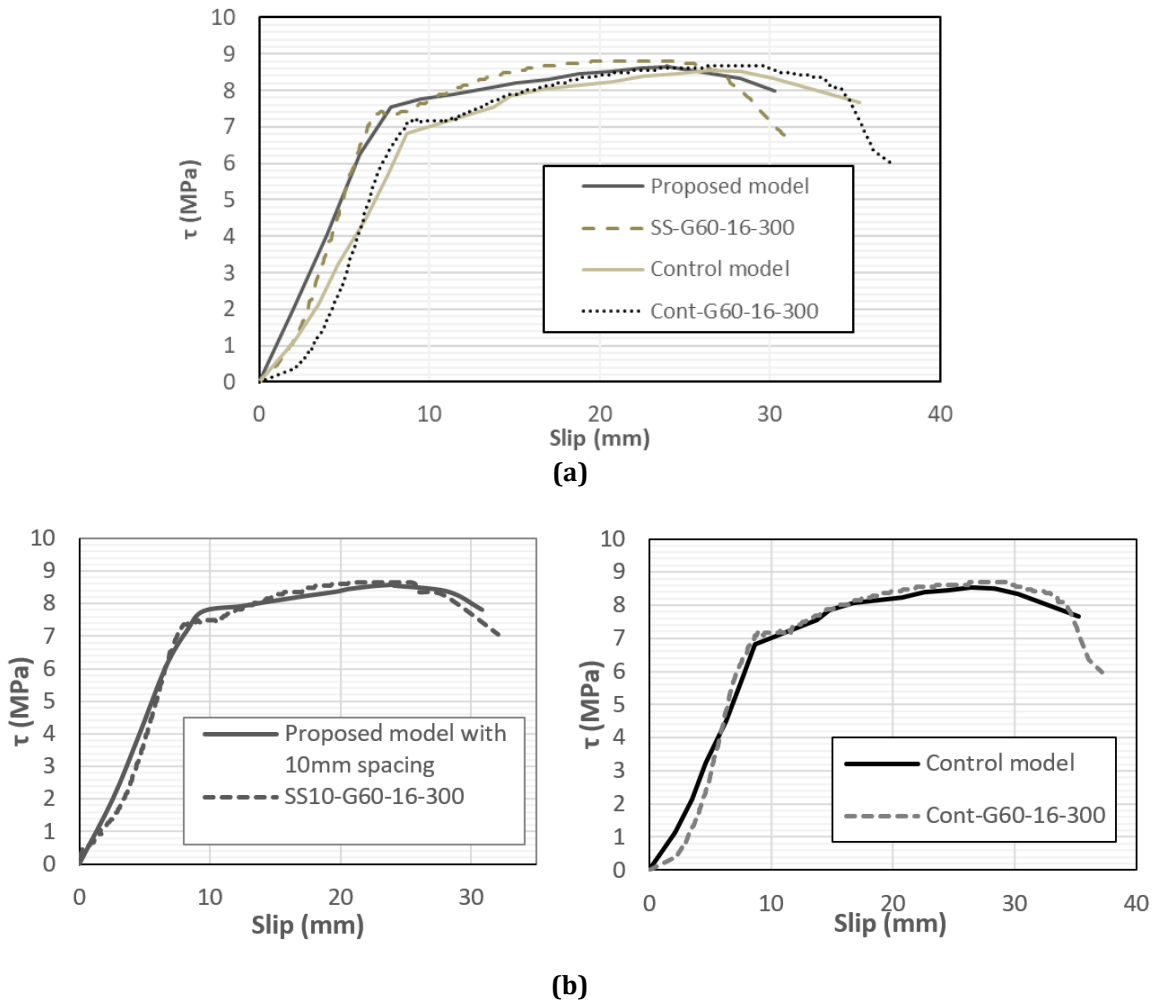


Fig. 6 Bond-slip curves of proposed models (a) Bond-slip curves of proposed model specimens; and (b) Bond-slip curves of proposed model with 10 mm spacing and control model

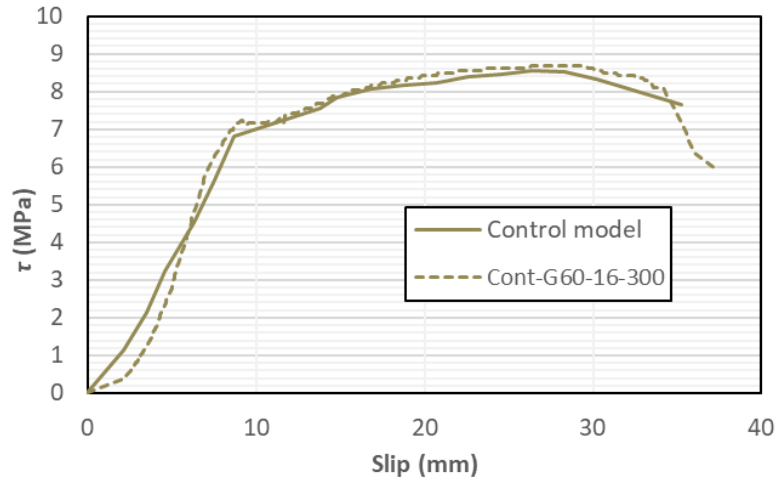


Fig. 7 Bond-slip curve of control model

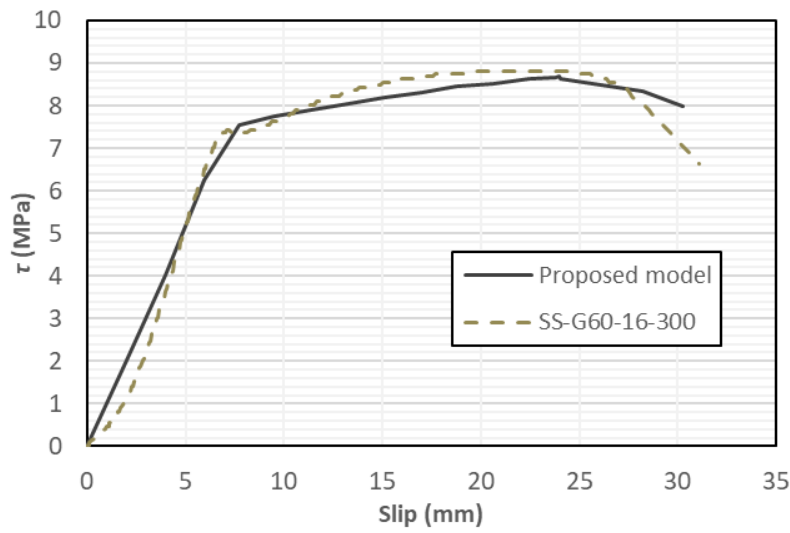


Fig. 8 Bond-slip curve of proposed model

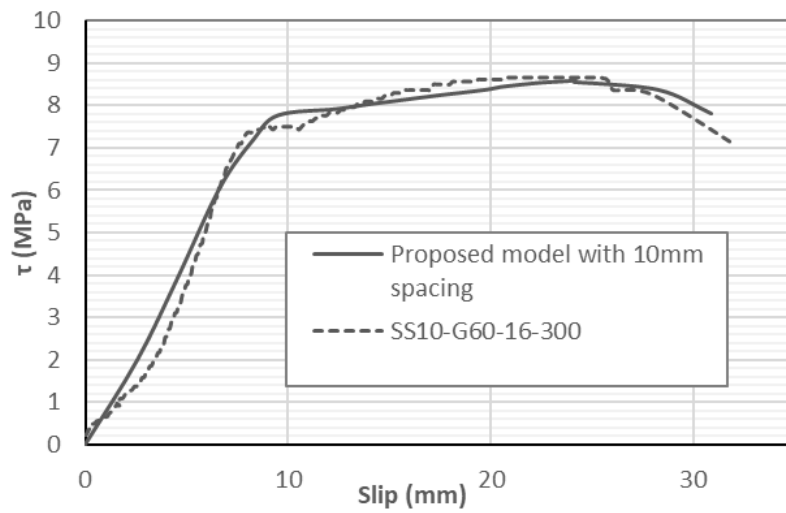


Fig. 9 Bond-slip curve of proposed model with 10 mm spacing

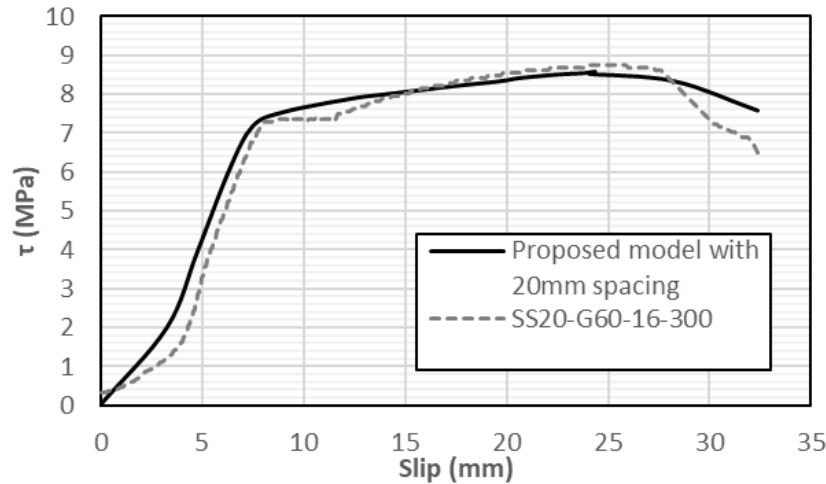


Fig. 10 Bond-slip curve of proposed model with 20 mm spacing

From Fig. 7, the control model has followed the trend of bond-slip curve exhibited by Cont-G60-16-300. It also can be seen for proposed model whereas the proposed bond-slip curve has predicted the bond-slip curve like the trend curve of SS-G60-16-300. The developed model curves have significantly predicted similar bond-slip curves of experimental curves.

From Fig. 9, the proposed model with 10 mm spacing predicted the bond-slip with similar trend to SS10-G60-16-300. The provision of ρ_v up to 0.14 has significantly predicted the bond-slip curve of confined concrete to be less than 5% compared to SS10-G60-16-300. Meanwhile, the proposed model with 20 mm spacing has predicted bond strength approximately less than 5% compared to SS20-G60-16-300. This indicated that the developed models can effectively predict the bond-slip curves of confined concrete.

It is worth noting that these models are developed based on the assumptions stated in Section 1. These assumptions formed the foundation for the model's development and analysis. While these assumptions are common in FEM, they may not fully represent the real-world structural behavior. Such simplifications could influence the accuracy of predicted results, especially in scenarios where anisotropic effects or bond deterioration play a significant role, or during uneven tensioning or incomplete contact during installation. Future work may consider incorporating more advanced material models and interface definitions to improve the model's fidelity to real-world conditions.

4. Conclusions

From the results, the following conclusions could be listed:

- The development of the FE model depends largely on the inputs by users in which these data influenced the accuracy of developed model. The bond-slip model of SSTT confinement is the first FE model that has ever been developed for predicting bond-slip curves of confined concrete.
- The proposed model and control model indicated that the effects of confinement have increased the elastic region of confined concrete compared to control up to 5%.
- The proposed model and control model have predicted the bond-slip curves of SS-G60-16-300 and Cont-G60-16-300 with 1.0% and 1.5% discrepancy, respectively.
- The proposed model has predicted the post-peak strength with about 15% higher compared to the post-peak strength exhibited by SS-G60-16-300. Moreover, the bar slipped by proposed model also reduced by 6.8% compared to SS-G60-16-300.
- The inclusion of ρ_v up to 0.152 in proposed model has increased the elastic properties of bond-slip curve by about 5% compared to control model. The proposed model has accurately predicted bond-slip curve of confined concrete for experimental bond-slip curve of SS-G60-16-300. Therefore, the proposed SSTT-confined model can be used to predict the bond-slip curves under confinement effects.

Although the proposed model has been validated via the available experimental results, the scope of validation would still remain limited. Future work should include the following:

- Additional experimental tests with varying parameters such as concrete strength, reinforcement size, and confinement intensity to further verify the model's predictive capability across a wider range of conditions.
- Long-term effects such as creep, shrinkage, and environmental degradation, which may significantly influence bond performance over time, were not considered. Future work should aim to incorporate time-dependent models and durability-based parameters to extend the applicability of the model to real-life service conditions.
- Parameter sensitivity studies to assess the influence of key variables on the model's predictive performance and ensure greater robustness.

Acknowledgement

The authors gratefully acknowledge the financial support received from the Universiti Teknologi Malaysia (UTM) Grant no: Q.J130000.5022.10G21 and Q.J130000.5022.10G22.

Conflict of Interest

Authors declare that there is no conflict of interests regarding the publication of the paper.

Author Contribution

The authors confirm contribution to the paper as follows: **study conception and design:** Muhd Fauzy Sulaiman, Chau-Khun Ma, Nazirah Mohd Apandi, Chee-Loong Chin; **data collection:** Muhd Fauzy Sulaiman, Chau-Khun Ma, Nazirah Mohd Apandi, Chee-Loong Chin; **analysis and interpretation of results:** Muhd Fauzy Sulaiman, Chau-Khun Ma, Nazirah Mohd Apandi, Chee-Loong Chin, Kee-Hong Ler; **draft manuscript preparation:** Muhd Fauzy Sulaiman, Chau-Khun Ma, Nazirah Mohd Apandi, Chee-Loong Chin, Kee-Hong Ler. All authors reviewed the results and approved the final version of the manuscript.

References

- [1] Azimi, M., Bagherpourhamedani, A., Tahir, M., Sam, A. R. & Ma, C. K. (2016) Evaluation of new spiral shear reinforcement pattern for reinforced concrete joints subjected to cyclic loading, *Advances in Structural Engineering*, 19(5), 730-745, <https://doi.org/10.1177/1369433216630371>
- [2] Bamonte, P., Coronelli, D. & Gambarova, P. G. (2004) Local bond stress-slip law and size effect in high-bond bars. Proc., 5th Int. Conf. on Fracture Mechanics of Concrete and Concrete Structures (FraMCoS-5), 2, 869-876.
- [3] Chen, H., Huang, C. & Kao, Z. (2004). Experimental investigation on steel-concrete bond in lightweight and normal weight concrete, *Structural Engineering and Mechanics*, 17(2), 141-152, <https://doi.org/10.12989/sem.2004.17.2.141>
- [4] Choi, E. S., Lee, J. W., Kim, S. J. & Kwark, J. W. (2015) A Study on the Bond Strength between High Performance Concrete and Reinforcing Bar, *Engineering*, 7(7), 373-378, <https://doi.org/10.4236/eng.2015.77033>
- [5] Sulaiman, M. F., Redzuan, F. A., Ma, C. K., Awang, A. Z. & Omar, W. (2017) Bond Between SSTT Confined Concrete and Ribbed Steel Reinforcement Bar, *Transactions on Science and Technology*, 4(3), 194-201
- [6] Sulaiman, M.F., Chin, C.L., Ma, C.K., Awang, A. Z. & Omar, W. (2022) Pullout Behaviour of Bars in Concrete Confined with Post-tensioned Steel Straps, *International Journal of Civil Engineering*, 20, 709-720, <https://doi.org/10.1007/s40999-021-00690-0>
- [7] Sulaiman, M. F., Chin, C. L., Ma, C. K., Awang, A. Z. & Omar, W. (2022) The bond strength of reinforced concrete with confinement of recycled steel strap, *Journal of Cleaner Production*, 369, 133352, <https://doi.org/10.1016/j.jclepro.2022.133352>
- [8] Wang, M., Wang, Y., Zhang, X. & Chen, G. (2024) Bond behavior and Bond Strength Model for ribbed FRP bar in FRP-confined concrete, *Construction and Building Materials*, 449, 138318, <https://doi.org/10.1016/j.conbuildmat.2024.138318>
- [9] Apandi, N. M., Ma, C. K., Chin, C. L., Awang, A. Z., Omar, W., Rashid, A., Safuan, A., Zailani, A. & Warid, W. (2023) Preliminary pre-damaged level assessment for concrete structures: a review, *Structures*, 11, 97-109, <https://doi.org/10.1016/j.istruc.2017.04.004>
- [10] Ler, K. H., Ma, C. K., Chin, C. L. & Goh, Y. Z. (2025) Concrete strengthening with external prestressed metal straps: A critical review, *Structural Concrete*, 26(4), <https://doi.org/10.1002/suco.202400449>

- [11] Azzam, A. (2025) A review on the effectiveness of FRP and hybrid wrappings for strengthening concrete columns. *Results in Engineering*, 27, 106023, <https://doi.org/10.1016/j.rineng.2025.106023>
- [12] Chin, C. L., Ma, C. K., Awang, A. Z., Tan, J. Y., Ong, C. B. & Omar, W. (2019) Confining stress path dependent stress-strain model for pre-tensioned steel-confined concrete, *Engineering Structures*, 201, 109769, <https://doi.org/10.1016/j.engstruct.2019.109769>
- [13] Neupane, R.P., Imjai, T. & Garcia, R. (2025) A novel post-tensioned metal strapping technique to actively confine concrete structures: a review, *Innovative Infrastructure Solutions*, 10, 16, <https://doi.org/10.1007/s41062-024-01791-0>
- [14] Seok, S., Haikal, G., Ramirez, J. A., Lowes, L. N. & Lim, J. (2020) Finite element simulation of bond-zone behavior of pullout test of reinforcement embedded in concrete using concrete damage-plasticity model 2 (CDPM2), *Engineering Structures*, 221, 110984, <https://doi.org/10.1016/j.engstruct.2020.110984>
- [15] Minh, H. L., Khatir, S., Wahab, M. A. & Cuong-Le, T. (2021) A concrete damage plasticity model for predicting the effects of compressive high-strength concrete under static and dynamic loads, *Journal of Building Engineering*, 44, 103239, <https://doi.org/10.1016/j.jobe.2021.103239>
- [16] Lin, H., Zeng, H., Feng, P., Jiang, C. & Zhang, Y. (2023) Bond behavior of FRP-concrete wet-bonding interface under lateral confinement. *Engineering Structures*, 292, 116536, <https://doi.org/10.1016/j.engstruct.2023.116536>
- [17] Chin, C. L., Ong, C. B., Tan, J. Y., Ma, C. K., Awang, A. Z. & Omar, W. (2020) Confinement-concrete interaction in pre-tensioned partial steel-confined concrete, *Structures*, 23, 751-765, <https://doi.org/10.1016/j.istruc.2019.12.006>
- [18] Lim, J. C., & Ozbakkaloglu, T. (2015) Unified stress-strain model for FRP and actively confined normal-strength and high-strength concrete, *Journal of Composites for Construction*, 19(4), 04014072, [https://doi.org/10.1061/\(ASCE\)CC.1943-5614.0000536](https://doi.org/10.1061/(ASCE)CC.1943-5614.0000536)
- [19] Ozbakkaloglu, T. & Akin, E. (2012) Behavior of FRP-confined normal-and high-strength concrete under cyclic axial compression, *Journal of Composites for Construction*, 16(4), 451-463, [https://doi.org/10.1061/\(ASCE\)CC.1943-5614.0000273](https://doi.org/10.1061/(ASCE)CC.1943-5614.0000273)
- [20] Ma, C. K., Awang, A. Z. & Omar, W. (2014) New theoretical model for SSTT-confined HSC columns, *Magazine of Concrete Research*, 66(13), 674-684, <https://doi.org/10.1680/marc.13.00230>
- [21] Arruda, M.R., Firmo, J.P., Correia, J.R. & Tiago, C. (2016) Numerical modeling of the bond between concrete and CFRP laminates at elevated temperatures, *Engineering Structures*, 110, 233-243, <https://doi.org/10.1016/j.engstruct.2015.11.036>